

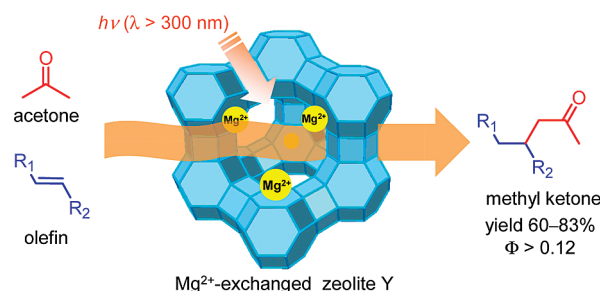
Highly Efficient Methyl Ketone Synthesis with Photoactivated Acetone and Olefins Assisted by Mg(II)-Exchanged Zeolite Y

Daijiro Tsukamoto, Yasuhiro Shiraishi,* and Takayuki Hirai

Research Center for Solar Energy Chemistry and Division of Chemical Engineering, Graduate School of Engineering Science, Osaka University, Toyonaka 560-8531, Japan

shiraish@cheng.es.osaka-u.ac.jp

Received October 31, 2009



We previously found that photoirradiation of an acetone/water mixture containing olefins affords the corresponding methyl ketones highly efficiently and selectively via a water-assisted C–C coupling between the acetyl radical and olefins (*Org. Lett.* **2008**, *10*, 3117–3120). The reaction proceeds at room temperature without any additives and has a potential to be a powerful method for methyl ketone synthesis. Here we report that an addition of Mg²⁺-exchanged zeolite Y (MgY) to the above photoreaction system accelerates the methyl ketone formation, while maintaining high selectivity. Ab initio molecular orbital calculation reveals that the accelerated methyl ketone formation is due to the electrostatic interaction between Mg²⁺ and excited-state acetone. This leads to a charge polarization of the carbonyl moiety of excited-state acetone and accelerates the hydrogen abstraction from ground-state acetone (acetyl radical formation). This promotes efficient addition of the acetyl radical to olefins, resulting in methyl ketone formation enhancement. Adsorption experiments reveal that accumulation of olefins inside the zeolite pore also affects efficient radical addition to olefins. The present process successfully produces various methyl ketones with very high yield, and the MgY recovered can be reused for further reaction without loss of activity.

1. Introduction

Ketone is one of the most important chemicals in the synthesis of natural products and pharmaceutical materials. Traditional alcohol oxidation processes require stoichiometric amounts of inorganic oxidants with concomitant formation of copious heavy-metal waste.¹ Recent advances in oxidation catalysts allow clean alcohol oxidation with

molecular oxygen,² but these processes require noble metal catalysts. Other ketone synthesis methods, such as Wacker oxidation³ and Suzuki–Miyaura cross-coupling,⁴ also require Pd-based catalysts. Development of new ketone synthesis methods with inexpensive reactants and catalysts is therefore currently in focus.

Earlier, we proposed a photochemical process for methyl ketone synthesis with acetone and olefins as reactants.⁵

*To whom correspondence should be addressed. Fax: +81-6-6850-6273. Tel: +81-6-6850-6271.

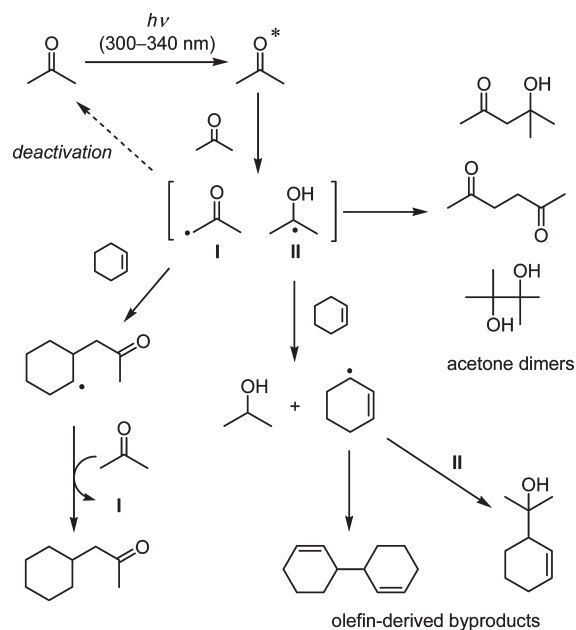
(1) (a) Cainelli, G.; Cardillo, G. *Chromium Oxidants in Organic Chemistry*; Springer: Berlin, Germany, 1984. (b) Ley, S. V.; Madin, A. In *Comprehensive Organic Synthesis*; Trost, B. M., Fleming, I., Ley, S. V., Eds.; Pergamon: Oxford, UK, 1991; Vol. 7, p 251.

(2) (a) ten Brink, G.-J.; Arends, I. W. C. E.; Sheldon, R. A. *Science* **2000**, *287*, 1636–1639. (b) Graves, C. R.; Zeng, B.-S.; Nguyen, S. T. *J. Am. Chem. Soc.* **2006**, *128*, 12596–12597. (c) Schultz, M. J.; Park, C. C.; Sigman, M. S. *Chem. Commun.* **2002**, 3034–3035.

(3) (a) Cornell, C. N.; Sigman, M. S. *Inorg. Chem.* **2007**, *46*, 1903–1909. (b) Cornell, C. N.; Sigman, M. S. *J. Am. Chem. Soc.* **2005**, *127*, 2796–2797. (c) Mitsudome, T.; Umetani, T.; Nosaka, N.; Mori, K.; Mizugaki, T.; Ebitani, K.; Kaneda, K. *Angew. Chem., Int. Ed.* **2006**, *45*, 481–485. (d) ten Brink, G.-J.; Arends, I. W. C. E.; Papadogianakis, G.; Sheldon, R. A. *Chem. Commun.* **1998**, 2359–2360.

(4) Miyaura, N.; Suzuki, A. *Chem. Rev.* **1995**, *95*, 2457–2483.

(5) Shiraishi, Y.; Tsukamoto, D.; Hirai, T. *Org. Lett.* **2008**, *10*, 3117–3120.

SCHEME 1. Mechanism of Methyl Ketone Formation with Photoactivated Acetone and Olefin


Photoirradiation (300–340 nm) of an acetone/water (6/4 v/v) mixture containing olefins at room temperature affords the corresponding methyl ketones highly selectively. The reaction proceeds via the following mechanism, as summarized in Scheme 1. The reaction is initiated by photoexcitation of acetone. The excited-state acetone promotes an intermolecular hydrogen abstraction (H-abstraction) from ground-state acetone and produces an acetonyl (**I**) and 2-hydroxy-2-propyl radical (**II**) pair.⁶ Most of these radical pairs undergo fast recombination (deactivation to ground-state acetones) or dimerization (formation of acetone dimers).^{6,7} The methyl ketone is produced by an addition of radical **I** to olefin followed by H-abstraction from ground-state acetone. In contrast, radical **II** reacts with olefin and produces olefin-derived byproducts. Addition of 40% water to this system, however, suppresses the formation of acetone dimers and olefin-derived byproducts. The water addition leads to a hydration of the respective radicals (**I** and **II**) and suppresses their dimerization. In that, the radical **II** is strongly hydrated and thus suppresses the formation of olefin-derived byproducts. These water effects therefore enable selective methyl ketone formation. The photoprocess exhibits significant advantages: (i) noble metal-free, (ii) cheap reactant (acetone), (iii) mild reaction condition (room temperature). This process, therefore, has a potential to be one of the powerful methods for methyl ketone synthesis.

The purpose of the present work is the acceleration of methyl ketone production in the above photoprocess. As shown in Scheme 1, the methyl ketone forms via the addition of radical **I** to olefins, where radical **I** is produced via the intermolecular H-abstraction from ground-state acetone by excited-state acetone. Radical **I** is, however, more or less deactivated by the recombination of radical pairs.^{6,7} The

enhancement of the radical **I** formation (enhancement of H-abstraction by excited-state acetone from ground-state acetone) is therefore one of the possible ways to accelerate the methyl ketone formation. There are, however, only a few reports of acceleration of intermolecular H-abstraction by excited-state carbonyl compounds.⁸ Dedinas et al.^{8a} and Boate et al.^{8b} reported that H-abstraction by the lowest triplet excited-state (T_1) decafluorobenzophenone from 2-propanol or cyclohexane occurs much faster than that by unmodified benzophenone. This is due to the enhanced charge polarization of the T_1 carbonyl group upon fluorine substitution. This implies that enhancement of charge polarization of excited-state acetone is one of the ways to accelerate the H-abstraction from ground-state acetone, although no specific method to promote charge polarization of excited-state carbonyl compounds has been reported until now.

A few pieces of literature reported the interaction between carbonyl compounds and metal cations. Ramamurthy and Turro⁹ reported that ground-state carbonyl compounds interact with alkali metal cations within zeolite Y (cation–carbonyl interaction). This electrostatic interaction leads to an increase in the electron density of the carbonyl oxygen, resulting in a charge polarization of the carbonyl group.¹⁰ Shailaja et al.¹¹ also studied the effect of alkali cations on the properties of excited-state acetophenone and clarified that T_1 acetophenone shows a $\pi\pi^*$ character within Na^+ -exchanged zeolite Y, while showing an $n\pi^*$ character in a bulk nonpolar solvent. Computational study revealed that this is due to the stabilized carbonyl n orbital of the T_1 acetophenone by a cation–carbonyl interaction. These findings imply that excited-state acetone, if interacted with metal cations electrostatically, may lead to a charge polarization of the carbonyl group. This may accelerate the H-abstraction from ground-state acetone and enable efficient production of radical **I**.

In the present work, effects of metal cations on the photochemical methyl ketone production have been studied. We found that addition of Mg^{2+} -exchanged zeolite Y (MgY) successfully enhances the methyl ketone production, while maintaining high selectivity. Ab initio molecular orbital calculation revealed that, as we expected, the enhanced methyl ketone formation is due to the electrostatic interaction between Mg^{2+} and excited-state acetone within the zeolite pore. We also describe here that accumulation of olefins inside the zeolite pore is also an important factor for efficient methyl ketone formation.

2. Results and Discussion

2.1. Effects of Cation-Exchanged Zeolite Y.

The effect of alkali and alkaline earth metal cation-exchanged zeolite Y on the methyl ketone formation was studied with 1-hexene (**1**) as

(6) Nakashima, M.; Hayon, E. *J. Phys. Chem.* **1971**, *75*, 1910–1914.

(7) (a) Shimizu, N.; Miyahara, T.; Mishima, M.; Tsuno, Y. *Bull. Chem. Soc. Jpn.* **1989**, *62*, 2032–2039. (b) Przybytek, J. T.; Singh, S. P.; Kagan, J. *J. Chem. Soc., Chem. Commun.* **1969**, 1224–1225.

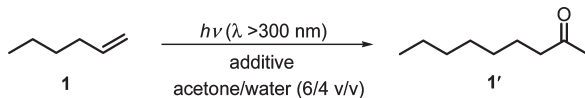
(8) (a) Dedinas, J.; Regan, T. H. *J. Phys. Chem.* **1972**, *76*, 3926–3933. (b) Boate, D. R.; Johnston, L. J.; Scaiano, J. C. *Can. J. Chem.* **1989**, *67*, 927–932. (c) Shoute, L. C. T.; Mittal, J. P. *J. Phys. Chem.* **1993**, *97*, 8630–8637.

(9) (a) Ramamurthy, V.; Turro, N. J. *J. Inclusion Phenom.* **1995**, *21*, 239–282.

(10) (a) Del Bene, J. E. *Chem. Phys.* **1979**, *40*, 329–335. (b) Raber, D. J.; Raber, N. K.; Chandrasekhar, J.; Schleyer, P. v. R. *Inorg. Chem.* **1984**, *23*, 4076–4080. (c) Guo, B. C.; Conklin, B. J.; Castleman, A. W., Jr. *J. Am. Chem. Soc.* **1989**, *111*, 6506–6510. (d) Remko, M. *Mol. Phys.* **1997**, *91*, 929–936.

(11) (a) Shailaja, J.; Lakshminarasimhan, P. H.; Pradhan, A. R.; Sunoj, R. B.; Jockusch, S.; Karthikeyan, S.; Uppili, S.; Chandrasekhar, J.; Turro, N. J.; Ramamurthy, V. *J. Phys. Chem. A* **2003**, *107*, 3187–3198. (b) Ramamurthy, V.; Shailaja, J.; Kaanumalle, L. S.; Sunoj, R. B.; Chandrasekhar, J. *J. Chem. Commun.* **2003**, 1987–1999.

TABLE 1. Results of the Photoreaction of 1 in an Acetone/Water Mixture with Various Additives^a



entry	additive	conversion of 1 (%)	GC yield of 1' (%)
1		67	47 ^b
2	LiY	97	69
3	NaY	93	65
4	KY	95	67
5	RbY	92	65
6	CsY	90	63
7	MgY	> 99	80 ^c
8	CaY	96	74
9	SrY	98	71
10	BaY	90	69
11	HY	80	56 ^d
12	MgMOR ^e	99	57
13	MgZSM-5 ^f	99	48
14	MgCl ₂ ^g	99	59
15	Mg(NO ₃) ₂ ^g	98	59

^aReaction conditions: acetone/water (6/4 v/v) mixture (10 mL), **1** (0.2 mmol), cation-exchanged zeolite Y (5 mg, containing ca. 2.6 μ mol alkali or alkaline earth cation), nitrogen (1 atm), $\lambda > 300$ nm, photoirradiation time (6 h). ^bMass balance was 81%, where 2-octanone (yield: 1.0%) and 2-methyl-2-octanol (0.5%) were produced as minor products. ^cMass balance was 82%, where 2-octanone (1.2%) and 2-methyl-2-octanol (0.7%) were also produced. ^dMass balance was 78%, where 2-octanone (0.9%) and 2-methyl-2-octanol (0.6%) were also produced. ^e5 mg (containing 1.6 μ mol Mg²⁺) was used. ^f5 mg (containing 1.0 μ mol Mg²⁺) was used. ^g26 μ mol of Mg salts was used.

a substrate. Table 1 (entries 2–10) summarizes the yields of 2-nonanone (**1'**) obtained by photoirradiation (Xe lamp, $\lambda > 300$ nm, 6 h) of an acetone/water mixture (6/4 v/v, 10 mL) containing **1** (20 mM) under nitrogen atmosphere with various cation-exchanged zeolite Y (5 mg). In that, the amount of alkali or alkaline earth cation on zeolite Y is ca. 5.2×10^{-4} mol g⁻¹. Without zeolite (entry 1), the yield of **1'** is 47%. Addition of alkali or alkaline earth metal cation-exchanged zeolite Y (entries 2–10) leads to an increase in the **1'** yield (> 63%). Among them, alkaline earth cations, especially lighter cations, show higher activity, where Mg²⁺-exchanged zeolite Y (MgY) shows the highest **1'** yield (80%, entry 7). As shown in entry 11, H⁺-exchanged zeolite Y (HY) shows low **1'** yield (56%), indicating that the **1'** production enhanced by alkali and alkaline earth cation-exchanged zeolite Y is mainly due to their cations. The zeolite Y framework is also important for efficient methyl ketone production. As shown in entries 12 and 13, the **1'** yields obtained with Mg²⁺-exchanged Mordenite (MgMOR, 57%) and ZSM-5 (MgZSM-5, 48%) are much lower than that obtained with MgY (80%). In addition, as shown in entries 14 and 15, the use of homogeneous Mg salts such as MgCl₂ and Mg(NO₃)₂ also shows low **1'** yields (59%). These results suggest that both Mg²⁺ and zeolite Y framework are necessary for efficient methyl ketone production.

As shown in Table 1, the **1'** yields are lower than the conversion of **1**, indicating that byproducts are produced during reaction. This is because, as shown in Scheme 1, several side reactions occur. GC-MS analysis detected some of the byproducts, such as 2-methyl-2-octanol and 2-octanone. The yields of these compounds are, however, much lower than those expected from the difference between the

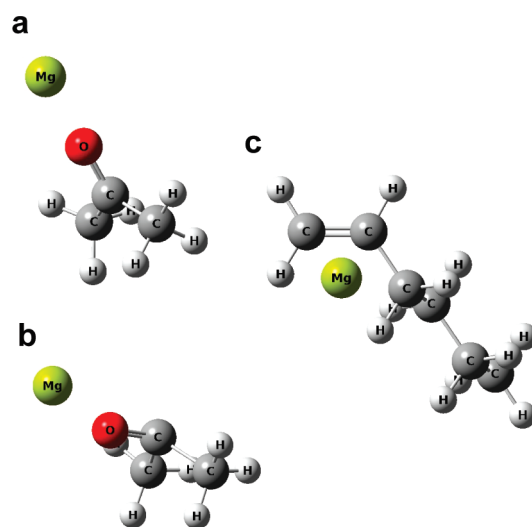


FIGURE 1. Optimized geometry of (a) S₀ acetone...Mg²⁺, (b) T₁ acetone...Mg²⁺, and (c) S₀ 1-hexene (**1**)...Mg²⁺ systems.

conversion of **1** and the **1'** yield (see footnote of Table 1). This suggests that nonvolatile or thermally degradable compounds such as carboxylic acids are the main byproducts. However, it must be noted that the product methyl ketone (**1'**) is not decomposed by prolonged photoirradiation. This indicates that the byproducts are not derived from the product methyl ketone.

2.2. Electrostatic Interaction between Excited-State Acetone and Cations. As reported,⁸ the H-abstraction by T₁ decafluorobenzophenone from alcohols and alkanes occurs faster than that by T₁ benzophenone because the fluorine substitution promotes charge polarization of the carbonyl group. It is also reported that ground-state carbonyl compounds interact with alkali metal cations within zeolite Y and this electrostatic cation–carbonyl interaction promotes a charge polarization of the carbonyl group.^{9,10} These results imply that, in the present photoprocess, excited-state acetone may interact with metal cations and promote charge polarization of the acetone carbonyl. This probably accelerates the H-abstraction from ground-state acetone (efficient production of radical **I**) and accelerates the methyl ketone formation (Table 1). To confirm this assumption, ab initio molecular orbital calculation was performed with the Gaussian 03 programs.¹² A simple modeling system consisting of a free metal cation and S₀ or T₁ acetone (Figure 1a,b)¹³ was

(12) (a) Frisch, M. J.; Trucks, G. W.; Schlegel, H. B.; Scuseria, G. E.; Robb, M. A.; Cheeseman, J. R.; Montgomery, J. A., Jr.; Vreven, T.; Kudin, K. N.; Burant, J. C.; Millam, J. M.; Iyengar, S. S.; Tomasi, J.; Barone, V.; Mennucci, B.; Cossi, M.; Scalmani, G.; Rega, N.; Petersson, G. A.; Nakatsuji, H.; Hada, M.; Ehara, M.; Toyota, K.; Fukuda, R.; Hasegawa, J.; Ishida, M.; Nakajima, T.; Honda, Y.; Kitao, O.; Nakai, H.; Klene, M.; Li, X.; Knox, J. E.; Hratchian, H. P.; Cross, J. B.; Bakken, V.; Adamo, C.; Jaramillo, J.; Gomperts, R.; Stratmann, R. E.; Yazyev, O.; Austin, A. J.; Cammi, R.; Pomelli, C.; Ochterski, J. W.; Ayala, P. Y.; Morokuma, K.; Voth, G. A.; Salvador, P.; Dannenberg, J. J.; Zakrzewski, V. G.; Dapprich, S.; Daniels, A. D.; Strain, M. C.; Farkas, O.; Malick, D. K.; Rabuck, A. D.; Raghavachari, K.; Foresman, J. B.; Ortiz, J. V.; Cui, Q.; Baboul, A. G.; Clifford, S.; Cioslowski, J.; Stefanov, B. B.; Liu, G.; Liashenko, A.; Piskorz, P.; Komaromi, I.; Martin, R. L.; Fox, D. J.; Keith, T.; Al-Laham, M. A.; Peng, C. Y.; Nanayakkara, A.; Challacombe, M.; Gill, P. M. W.; Johnson, B.; Chen, W.; Wong, M. W.; Gonzalez, C.; and Pople, J. A. *Gaussian 03*, Revision B.05; Gaussian, Inc., Wallingford, CT, 2004. (b) Dennington, R., II; Keith, T.; Millam, J.; Eppinnett, K.; Hovell, W. L.; Gilliland, R. *GaussView*, Version 3.09; Semichem, Inc., Shawnee Mission, KS, 2003.

(13) Sunoj, R. B.; Lakshminarasimhan, P.; Ramamurthy, V.; Chandrasekar, J. J. *Comput. Chem.* **2001**, *22*, 1598–1604.

TABLE 2. Calculated Binding Affinities (ΔE) and Distances between Metal Cations and S_0 Acetone, T_1 Acetone, or S_0 1-Hexene (1)^a

cations	S_0 acetone		T_1 acetone		S_0 1-hexene (1)	
	ΔE (kcal mol ⁻¹) ^b	distance (Å) ^c	ΔE (kcal mol ⁻¹) ^b	distance (Å) ^c	ΔE (kcal mol ⁻¹) ^b	distance (Å) ^d
Mg ²⁺	118.9	1.84	75.5	1.88	87.7	2.19
Ca ²⁺	80.8	2.21	38.1	2.21	46.1	2.66
Sr ²⁺	66.4	2.42	23.8	2.40	32.8	2.95
Ba ²⁺	56.9	2.62	32.1	2.74	25.5	3.19
Li ⁺	48.8	1.79	29.5	1.90	23.8	2.21
Na ⁺	35.1	2.18	20.5	2.30	16.4	2.63
K ⁺	25.5	2.55	14.2	2.66	9.0	3.07
Rb ⁺	21.0	2.83	11.3	2.96	6.5	3.47
Cs ⁺	18.2	3.06	9.6	3.11	5.1	3.74

^aCalculations were performed at the MP2/6-31+G(d) level for H, C, O, Li, Na, K, Mg, and Ca and at the MP2/LAVCP* level for Rb, Cs, Sr, and Ba. ^b $\Delta E = E(\text{molecule} \cdots M^{n+}) - (E(\text{molecule}) + E(M^{n+}))$, where E denotes the SCF energies. ^cThe core–core distance between metal cation and carbonyl oxygen. ^dThe distance between the metal cation and the C=C bond of **1**. Cartesian coordinates of the respective systems and the data for $E(\text{molecule} \cdots M^{n+})$ are summarized in the Supporting Information.

employed for the calculation. Table 2 summarizes the binding affinities between cations and S_0 or T_1 acetone, calculated based on the second order Møller–Plesset (MP2) theory.¹⁴ The binding affinities for both S_0 and T_1 acetones increase with cations in the following order: Mg²⁺ > Ca²⁺ > Sr²⁺ > Ba²⁺ > Li⁺ > Na⁺ > K⁺ > Rb⁺ > Cs⁺. This indicates that both S_0 and T_1 acetones strongly associate with alkaline earth cations, especially lighter cations, with the strongest affinity with Mg²⁺. This trend is consistent with the trend of **1'** yield (Table 1) obtained by reaction with various cation-exchanged zeolite Y (Mg²⁺ > Ca²⁺ > Sr²⁺ > Ba²⁺ ≈ Li⁺ > K⁺ > Na⁺ ≈ Rb⁺ > Cs⁺). These data indicate that the electrostatic affinity between the ground- or excited-state acetone and metal cations is closely related to the efficiency of methyl ketone formation.

Figure 2 summarizes the electron densities of carbonyl carbon and oxygen atoms of T_1 acetone, when interacted with the respective cations. Upon interaction with cations, the electron densities of carbonyl carbon decrease, while those of carbonyl oxygen increase. This indicates that electrostatic interaction with cations indeed leads to a charge polarization of the T_1 acetone carbonyl. The difference between the electron densities of carbonyl carbon and oxygen of T_1 acetone becomes more apparent when interacted with alkaline earth cations, especially Mg²⁺, in the order of

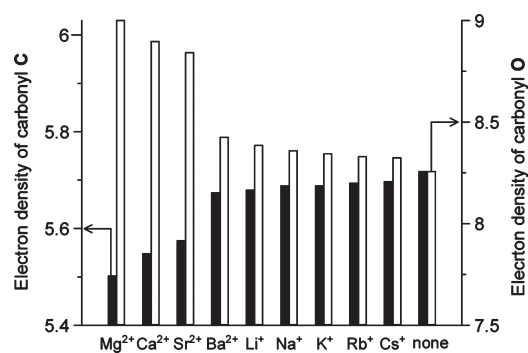


FIGURE 2. Calculated electron densities of carbonyl carbon and oxygen atoms of T_1 acetone, when interacted with alkali or alkaline earth cations. The electron densities of S_0 acetone when interacted with cations are shown in Figure S1 (Supporting Information). The detailed calculation data are summarized in Table S1 (Supporting Information).

Mg²⁺ > Ca²⁺ > Sr²⁺ > Ba²⁺ > Li⁺ > Na⁺ ≈ K⁺ > Rb⁺ > Cs⁺. This trend is almost consistent with the trend of **1'** yield (Table 1). As reported,⁸ charge polarization of T_1 carbonyl compounds accelerates the intermolecular H-abstraction. The above calculation results clearly indicate that the electrostatic interaction between Mg²⁺ and excited-state acetone enhances the charge polarization of acetone carbonyl and, hence, accelerates the H-abstraction from ground-state acetone. This therefore promotes efficient radical **I** formation and enhances the methyl ketone formation. As reported,¹¹ hydrated zeolite makes the interaction of the cations with guest molecules ineffective. However, the experimental results (Table 1) and the calculation results (Figure 2) indicate that, in the present process, the acetone molecules indeed interact with Mg²⁺ within zeolite even in the hydrated conditions.¹⁵

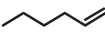

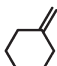


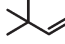

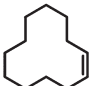
It is well-known that alkali and alkaline earth cations interact with the π electron of olefins (cation– π interaction).¹¹ Clark¹⁶ reported that efficient alkyl radical addition to ethylene in the gas phase with Li⁺-exchanged zeolite Y is due to the cation– π interaction between Li⁺ and ethylene, which decreases the activation energy of the radical addition. This implies that, also in our photoprocess, the cation– π interaction between Mg²⁺ and olefins is likely to contribute to the

(14) (a) Head-Gordon, M.; Pople, J. A.; Frisch, M. J. *Chem. Phys. Lett.* **1988**, *153*, 503–506. (b) Frisch, M. J.; Head-Gordon, M.; Pople, J. A. *Chem. Phys. Lett.* **1990**, *166*, 275–280. (c) Frisch, M. J.; Head-Gordon, M.; Pople, J. A. *Chem. Phys. Lett.* **1990**, *166*, 281–290.

(15) Phosphorescence analysis usually provides important information on the nature of the excited-state carbonyl compounds within zeolite (ref 11). However, in the present case, the analysis does not provide clear information on the nature of excited-state acetone within MgY in the absence and presence of water. Figure S2 (Supporting Information) shows phosphorescence spectra of acetone measured at 77 K. In a diethyl ether/2-propanol glass, a distinctive emission assigned to acetone phosphorescence appears at 455 nm: Borkman, R. F.; Kearns, D. R. *J. Chem. Phys.* **1966**, *44*, 945–949. In contrast, acetone adsorbed on MgY shows a red-shifted emission at 493 nm. As reported in the following, the red-shifted emission is assigned to the phosphorescence of the protonated acetone formed by a reaction with acidic hydroxyl groups on zeolite: Bosacek, V.; Kubelkova, L. *Zeolites* **1990**, *10*, 64–65. A similar emission red shift is observed on highly acidic HY. In contrast, no emission red shift is observed on less acidic CsY: Okamoto, S.; Nishiguchi, H.; Anpo, M. *Chem. Lett.* **1992**, 1009–1012. These data support the protonation of acetone within MgY. Addition of water to the MgY sample leads to a blue shift of the emission ($\lambda_{\text{max}} = 467$ nm). This is probably because, as reported in the following, hydration of zeolite weakens its acidity and suppresses the protonation of acetone: Ward, J. J. *Phys. Chem.* **1968**, *72*, 4211–4213. These indicate that the zeolite acidity strongly affects the acetone phosphorescence. A clear explanation as to how the cation affects the nature of the excited acetone within zeolite in the absence and presence of water, therefore, cannot be made.

(16) (a) Clark, T. *J. Chem. Soc., Chem. Commun.* **1986**, 1774–1776. (b) Clark, T. *J. Am. Chem. Soc.* **2006**, *128*, 11278–11285.

TABLE 3. Cylindrical Dimensions of Olefins and Their Effect on the Methyl Ketone Formation Enhancement ($Y_{\text{MgY}}/Y_{\text{none}}$)

Olefins	length \times width (\AA) ^a	$Y_{\text{MgY}}/Y_{\text{none}}$ (-) ^{b,c}
 1	7.6 \times 4.2	1.70
 2	5.3 \times 4.9	1.30
 3	6.7 \times 5.6	2.73 ^d
 4	7.6 \times 6.0	1.94
 5	8.9 \times 5.1	1.37
 6	6.6 \times 5.0	1.43
 7	14.8 \times 5.8	0.90 ^e
 8	8.1 \times 8.0	1.02 ^e

^aDetermined according to a literature procedure (ref 17). ^bThe ratio of methyl ketone yields obtained with and without MgY. ^cReaction conditions: acetone/water (6/4 v/v) mixture (10 mL), olefin (0.2 mmol), MgY (5 mg), nitrogen (1 atm), $\lambda > 300$ nm, photoirradiation time (6 h). ^dPhotoirradiation time (2 h) was employed because 6 h of irradiation converts almost all of **3** even without MgY. ^e0.05 mmol of olefin was used because of low solubility in solution. The detailed results are summarized in Table S2 (Supporting Information).

methyl ketone formation enhancement. This possibility, however, can be ruled out by the following results. Table 2 shows the binding affinities between cations and 1-hexene (**1**) calculated with use of an $\mathbf{1} \cdot \cdot \cdot$ free cation system (Figure 1c). The affinity of **1** with Mg^{2+} (87.7 kcal mol⁻¹) is comparable to that of T₁ acetone (75.5 kcal mol⁻¹), but much lower than that of S₀ acetone (118.9 kcal mol⁻¹). This indicates that Mg^{2+} interacts with ground-state acetone more strongly than **1**. In addition, in the present photoprocess, a larger number of acetone molecules exist as compared to **1**, where the ratio of acetone/**1** is 410/1 (mol/mol). These data suggest that, in the present photoprocess, electrostatic interaction between cations and olefins is negligible. This therefore leaves the electrostatic interaction between cation and excited-state acetone and the corresponding H-abstraction enhancement as the predominant factor for methyl ketone formation enhancement.

2.3. Role of the Zeolite Y Framework. As shown in Table 1, MgMOR, MgZSM-5, and homogeneous Mg^{2+} salts are less effective, indicating that the zeolite Y framework is also important for efficient methyl ketone formation. Alkali or

alkaline earth cations exist within the supercage of zeolite Y,¹¹ meaning that the H-abstraction between excited- and ground-state acetones occurs inside the zeolite pores and produces radical **I** there. To clarify whether the addition of radical **I** to olefins occurs inside the zeolite pore or not, the effect of the size of olefins on the reaction was studied with various olefins (**1–8**). Table 3 shows the size of these olefins determined in terms of a minimum cylindrical dimension.¹⁷ The pore system of zeolite Y consists of a spherical supercage with a 13.4 Å diameter, connected through a window with a 7.6 Å diameter.¹¹ The length and width of **1–6** olefins are less than 8.9 Å and 5.4 Å, respectively, which are smaller than the diameter of supercage and window, respectively. This indicates that these olefins can diffuse into the pore of zeolite Y. In contrast, the length of **7** (14.8 Å) and the width of **8** (8.0 Å) are larger than the diameter of supercage and window, respectively, suggesting that these olefins are difficult to diffuse inside the pore.

(17) (a) Morkin, T. L.; Turro, N. J.; Kleinman, M. H.; Brindle, C. S.; Kramer, W. H.; Gould, I. R. *J. Am. Chem. Soc.* **2003**, *125*, 14917–14924. (b) Chen, Y.-Z.; Wu, L.-Z.; Zhang, L.-P.; Tung, C.-H. *J. Org. Chem.* **2005**, *70*, 4676–4681.

Table 3 shows the ratio of methyl ketone yields ($Y_{\text{MgY}}/Y_{\text{none}}$) obtained by photoreaction of respective olefins with and without MgY. In the case of small olefins (1–6), the $Y_{\text{MgY}}/Y_{\text{none}}$ ratio is larger than 1, indicating that methyl ketone formation is indeed enhanced with MgY. In contrast, the ratio for large olefins (7 and 8) is almost 1, indicating that MgY is ineffective for the reaction of these olefins. These suggest that small olefins can diffuse inside the zeolite pores and react efficiently with the radical **I** formed there, resulting in efficient methyl ketone formation. In contrast, large olefins are difficult to diffuse inside the pores and result in almost no acceleration of methyl ketone formation. These suggest that the uptake of olefins inside the MgY pores is an important factor for reaction enhancement.

The importance of olefin uptake inside the zeolite pore is further supported by adsorption experiments. This was performed by stirring an acetone/water (6/4 v/v) mixture containing the respective olefins with MgY at 298 K for 6 h. The degree of olefin adsorption onto MgY was defined as a distribution ratio, D ,¹⁸ as follows:

$$D = (C_0 - C_e)/C_e \quad (1)$$

where C_0 is the initial concentration of olefin in the solution and C_e is the equilibrium concentration of olefin in the solution. Figure 3 shows the relationship between D and the ratio of methyl ketone yield ($Y_{\text{MgY}}/Y_{\text{none}}$). The large size 7 and 8 olefins show low D (<0.10) and low $Y_{\text{MgY}}/Y_{\text{none}}$ (almost equal to 1) values. In contrast, the small size 1–6 olefins show high D (>0.68) and high $Y_{\text{MgY}}/Y_{\text{none}}$ values. These results indicate that the large olefins are difficult to diffuse inside the zeolite pore and, hence, are less adsorbed onto the internal zeolite surface. In contrast, small olefins can diffuse inside the pores and are adsorbed well.¹⁹ The small olefins accumulated inside the pores of MgY, therefore, react efficiently with radical **I** formed there, resulting in enhanced methyl ketone formation. These findings clearly suggest that the olefin accumulation inside the MgY pore also contributes to efficient methyl ketone formation.²⁰

As shown in Table 1, MgMOR and MgZSM-5 scarcely enhance the methyl ketone formation. This is because the narrow pore size of MOR and ZSM-5²¹ suppresses the diffusion of olefins and hence suppresses the addition of radical **I** to olefins. It is well-known that the effective pore size of zeolites is usually defined with the Spaciousness Index (SI), which is the ratio of isobutane/*n*-butane formed during

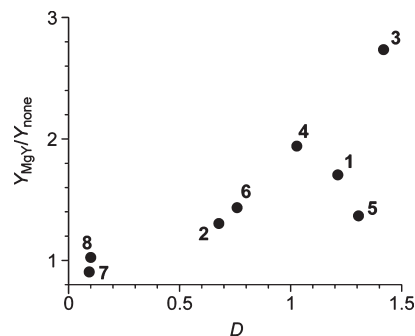
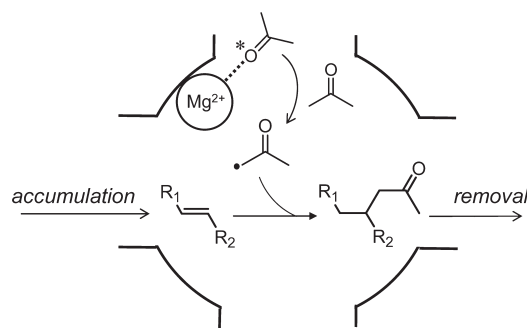


FIGURE 3. Relationship between distribution ratio, D , and the ratio of methyl ketone yields ($Y_{\text{MgY}}/Y_{\text{none}}$) obtained with and without MgY for reaction of the respective olefins (1–8). The detailed D data are summarized in Table S2 (Supporting Information).

SCHEME 2. Schematic Representation of the Mechanism of Methyl Ketone Formation within MgY



hydrocracking of *n*-butylcyclohexane.²² The SI values of MOR and ZSM-5 are 7.5 and 1.0, respectively, whereas the value of zeolite Y is more than 20. The adsorption test further confirms this. The distribution ratio, D , of **1** on MgMOR and MgZSM-5 is determined to be 0.06 and 0.01, respectively, whereas that on MgY is 1.21. This clearly indicates that, on MOR and ZSM-5, olefins are scarcely accumulated inside the pores. As shown in Table 1, homogeneous Mg salts are also ineffective for methyl ketone formation, indicating that the olefin accumulation within the MgY pore is significantly important for methyl ketone formation enhancement.

In the present process, the methyl ketones formed within the MgY pores successfully diffuse out to a bulk solution, while the olefins are accumulated. The distribution ratio, D , of the methyl ketones, **1'** (2-nonanone) and **2'** (1-cyclopentyl-2-propanone) on MgY, is very low (3.24×10^{-3} and 3.45×10^{-3}), while the values for the corresponding olefins **1** and **2** are very high (1.21 and 0.68). This is because ketones are more polar and have higher solubility in an aqueous solution than the corresponding olefins.²³ The mechanism of MgY-assisted methyl ketone formation can therefore be shown schematically in Scheme 2. The electrostatic interaction between Mg^{2+} and excited-state acetone accelerates the radical **I** formation. Radical **I** reacts efficiently with olefins accumulated inside the MgY pore and accelerates the methyl ketone formation. The methyl ketones formed smoothly diffuse out of the pores.

(18) Shiraishi, Y.; Saito, N.; Hirai, T. *J. Am. Chem. Soc.* **2005**, *127*, 12820–12822.

(19) Adsorption of substrates onto the solid surface depends on the affinity of substrates for the surface and the solubility of substrates in solvents: Wright, E. H. M.; Pratt, N. C. *J. Chem. Soc., Faraday Trans. 1* **1974**, *70*, 1461–1471. In the present case, acetone/water mixture has a poor solubility of olefins and, hence, allows olefin adsorption onto zeolite. This is confirmed by adsorption experiments of **1** with MgY (Figure S3; Supporting Information): the adsorption of **1** onto MgY in pure acetone is almost zero, but an increase in water content of the solution leads to an increase in the adsorption amount.


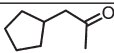
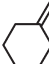
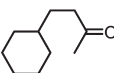
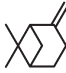
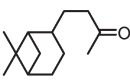

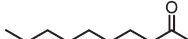
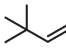
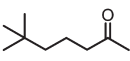
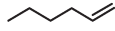
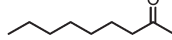
(20) It must be noted that, as shown in Table 3 and Figure 3, there is no linear relationship between the methyl ketone yield enhancement and the size or the adsorption degree of olefins. This suggests that the electronic structure of olefins (reactivity with the radical **I**) is also the important factor for methyl ketone production as well as the size and adsorption degree of olefins.

(21) Abbot, J.; Wojciechowski, B. W. *J. Catal.* **1984**, *90*, 270–278.

(22) (a) Weitkamp, J.; Ernst, S.; Kumar, R. *Appl. Catal.* **1986**, *27*, 207–210. (b) Chen, C.; Finger, L. W.; Medrud, R. C.; Kibby, C. L.; Crozier, P. A.; Chan, I. Y.; Harris, T. V.; Beck, L. W.; Zones, S. I. *Chem.—Eur. J.* **1998**, *4*, 1312–1323.

(23) Tewarl, Y. B.; Miller, M. M.; Waslk, S. P.; Martire, D. E. *J. Chem. Eng. Data* **1982**, *27*, 451–454.

TABLE 4. Effect of MgY on the Photochemical Methyl Ketone Formation^a

entry	catalyst	olefin	<i>t</i> (h)	conv. (%)	product	GC yield (%)	Φ (-) ^b
1			12	83		49	0.08
2	MgY	2	12	99	2'	76	0.12
3			2	33		15	0.14
4	MgY	3	2	64	3'	41	0.39
5	MgY	3	6	>99	3'	85	
6			6	60		33	0.10
7	MgY	4	6	84	4'	64	0.20
8			6	96		52	0.16
9	MgY	5	6	99	5'	71	0.22
10			6	55		44	0.14
11	MgY	6	6	70	6'	63	0.20
12			6	67		47	0.15
13	MgY		6	>99		80	0.25
14	MgY ^c	1	6	>99	1'	79	
15	MgY ^d		6	>99		80	

^aReaction conditions: acetone/water (6/4 v/v) mixture (10 mL), olefin (0.2 mmol), MgY (5 mg), nitrogen (1 atm), $\lambda > 300$ nm. ^bQuantum yields of the methyl ketone formation. ^cReused after run 13. ^dReused after run 14.

2.4. Synthesis of Various Methyl Ketones with MgY. As summarized in Table 4, the present photoprocess with MgY successfully produces various kinds of methyl ketones. Both acyclic and cyclic methyl ketones are produced with much higher yields as compared to that obtained without MgY. Quantum yields of the methyl ketone formation with MgY (0.12–0.39) are much higher than that obtained without MgY (0.08–0.16). The quantum yields are higher than those of other photochemical reactions for organic synthesis (< 0.07),²⁴ indicating that the present photoprocess proceeds highly efficiently. The MgY used in this process can easily be recovered by a simple centrifugation. As shown in entries 13–15, the MgY recovered can be reused without loss of activity at least twice. Applying the basic concept presented here with MgY may help realize methyl ketone synthesis in an economically and environmentally friendly way.

3. Conclusions

Effects of Mg²⁺-exchanged zeolite Y (MgY) on the photochemical methyl ketone synthesis with acetone and olefin as

reactants have been studied. The methyl ketone formation is much enhanced with MgY. This is due to the combination of electrostatic interaction between Mg²⁺ and excited-state acetone and accumulation of olefins inside the MgY pore. The electrostatic interaction between Mg²⁺ and excited-state acetone accelerates the H-abstraction from ground-state acetone and enhances the acetyl radical formation. In that, olefins with a size smaller than the zeolite pore are accumulated inside the pores and react efficiently with the acetyl radical formed there. The present process enables the synthesis of various kinds of methyl ketones, where MgY is reusable without loss of activity. The present photoprocess allows clean and efficient synthesis of methyl ketones with cheap reactants (olefin, acetone, water) and without noble metal catalysts. The basic concept presented here with MgY may become one of the powerful methods for methyl ketone synthesis.

4. Experimental Section

Materials. All of the materials used were of the highest commercial quality and were used without further purification. Commercially unavailable methyl ketones (**2'**, **3'**, **4'**, **6'**, and **8'**)

(24) Leigh, W. J.; Srinivasan, R. *Acc. Chem. Res.* **1987**, *20*, 107–114.

were synthesized according to a literature procedure²⁵ and used as standards for GC analysis. The details are summarized in the Supporting Information with the obtained NMR charts (Figures S4–S9). Alkali and alkaline earth metal cation-exchanged zeolite Y were synthesized according to a literature procedure²⁶ with NaY (Tosoh Corp.; HSZ-320NAA; SiO₂/Al₂O₃ = 5.5; BET surface area, 700 m² g⁻¹) as follows: NaY (3 g) was refluxed for 24 h in water (30 mL) containing 10 wt % respective metal salts (LiNO₃, KNO₃, RbCl, CsCl, MgCl₂, Ca(NO₃)₂, Sr(NO₃)₂, BaCl₂). The resulting solid was recovered by filtration, washed with water, and dried for 12 h at 100 °C. This procedure was repeated three times. MgMOR and MgZSM-5 were obtained in a similar manner, using NaMOR (Japan Reference Catalyst.; JRC-Z-M15; SiO₂/Al₂O₃ = 15; 426 m² g⁻¹) supplied from the Catalyst Society of Japan and NaZSM-5 (Tosoh Corp.; HSZ-820NAA; SiO₂/Al₂O₃ = 23.3; 340 m² g⁻¹). HY (Tosoh Corp.; HSZ-331HSA; SiO₂/Al₂O₃ = 6; 650 m² g⁻¹) was used as received.

Photoreaction. Each olefin was dissolved in an acetone/water mixture (6/4 v/v; 10 mL) within a Pyrex glass tube (ϕ 10 mm; capacity, 20 cm³). Zeolite material (5 mg) was added to the solution and dispersed well by ultrasonication for 5 min. The tube was sealed with a rubber septum cap, purged with nitrogen gas, and photoirradiated with magnetic stirring by a Xe lamp (2 kW; light intensity, 32.1 mW m⁻² at 300–340 nm). After the reaction, the sample was subjected to centrifugation, and the solution obtained was analyzed by GC-FID. The quantum yield for methyl ketone formation was determined with a *trans*-stilbene actinometer ($\Phi = 0.45$ in benzene),²⁷ where a 313 nm emission line was irradiated with a high-pressure Hg lamp (300 W, light intensity, 3.1 mW m⁻²),²⁸ filtered through a potassium chromate solution consisting of K₂CrO₄ (0.27 g L⁻¹) and K₂CO₃ (1 g L⁻¹).

Ab Initio Calculations. Calculations were performed with the Gaussian 03 program based on second-order Møller–Plesset

(MP2) theory.¹⁴ Geometries were fully optimized at the MP2/6-31+G(d) level for H, C, O, Li⁺, Na⁺, K⁺, Mg²⁺, and Ca²⁺ atoms and at the MP2/LAVCP* level for Rb⁺, Cs⁺, Sr²⁺, and Ba²⁺ atoms. Calculation of the T₁ acetone was performed using the basis set with the diffuse and polarization functions according to a literature procedure,²⁹ where the initial guess of T₁ acetone was generated by selecting an appropriate orbital occupancy and the nature of the electronic state was checked graphically with the molecular orbital.¹³ The optimized structure was then used for frequency calculation. The binding affinities were calculated with the MP2 theory according to a literature procedure,^{10a} without the basis set for superposition error corrections. The electron densities were determined by the natural population analysis.³⁰

Cylindrical Dimensions of Olefins. The length and width of olefins were determined according to a literature procedure using the MM2 program within the Chem3D-Pro software (CambridgeSoft, Inc.).¹⁷ Molecular dynamics annealing calculations were performed first to obtain a lowest energy structure, where the cooling rate was 1 kcal/atom/ps and the final temperature was 300 K, respectively. The minimization of the molecular energy was performed to a minimum rms gradient of 0.1. The relevant axes of the resulting structure were determined graphically, and 1.0 Å was added to these distances to take into account the dimensions of the exterior hydrogen atoms.

Acknowledgment. This work was supported by a Grant-in-Aid for Scientific Research (No. 19760536) from the Ministry of Education, Culture, Sports, Science and Technology, Japan (MEXT). We thank the Division of Chemical Engineering for the Lend-Lease Laboratory System.

Supporting Information Available: Synthesis of standard methyl ketones, supplementary data (Figures S1–S9 and Tables S1 and S2), and Cartesian coordinates and SCF energies for calculated structures. This material is available free of charge via the Internet at <http://pubs.acs.org>.

(25) Linker, U.; Kersten, B.; Linker, T. *Tetrahedron Lett.* **1995**, *51*, 9917–9926.

(26) Kaanumalle, L. S.; Shailaja, J.; Robbins, R. J.; Ramamurthy, V. *J. Photochem. Photobiol. A* **2002**, *153*, 55–65.

(27) Lewis, F. D.; Johnson, D. E. *J. Photochem.* **1977**, *7*, 421–423.

(28) Shiraiishi, Y.; Saito, N.; Hirai, T. *J. Am. Chem. Soc.* **2005**, *127*, 8304–8306.

(29) Foresman, J. B.; Head-Gordon, M.; Pople, J. A. *J. Phys. Chem.* **1992**, *96*, 135–149.

(30) Read, A. E.; Weinstock, R. B.; Weinhold, F. *J. Chem. Phys.* **1995**, *83*, 735–746.